

# Highly sensitive triangular photonic crystal fiber sensor design applicable for gas detection

# Aryan Abbaszadeh<sup>1</sup>, Somayeh Makouei<sup>1\*</sup>, and Saeed Meshqini<sup>2</sup>

1\*,1,2 Faculty of Electrical and Computer Engineering, University of Tabriz, Tabriz, 51664, Iran Corresponding author: Somayeh Makouei (e-mail: makouei@tabrizu.ac.ir).

**ABSTRACT** A new triangular photonic crystal fiber with a based microstructure core gas sensor has been proposed for the wavelength range from 1.1 µm to 1.7 µm. The guiding trait of the proposed structure depends on geometric parameters and wavelength, which are numerically studied by the finite element method. According to the results, the relative sensitivity obtained as high as 75.14% at 1.33µm wavelength. High birefringence and effective area are also obtained by order of 3.75×10<sup>-3</sup> and 14.07 μm<sup>2</sup>. Finally, a low confinement loss of 1.41×10<sup>-2</sup> dB/m is acquired at the same wavelength. The variation of the diameters in the cladding and core region is investigated, and the results show that this structure has good stability for manufacturing goals. Since the results show the highest sensitivity at wavelengths around 1.2 µm to 1.7 µm, which is the absorption line of many gases such as methane (CH<sub>4</sub>), hydrogen fluoride (HF), ammonia (NH3), this gas sensor can be used for medical and industrial applications.

**INDEX TERMS** Gas sensor, Photonic crystal fiber, Sensitivity.

## I. INTRODUCTION

Recently, photonic crystal fibers (PCFs) have opened a new era in communication and sensing applications. These fibers are made up of an alternating array [1] or regular arrangement [2] of microscopic holes in the air that are spread along with the fiber made of a silicone background. These fibers are divided into two categories based on the mechanism of light: Photonic Band-gap Fiber (PBG) [3] and Effective index-guide (IG) [4]. In band-gap fibers, light is moved by the law of the optical band gap inside the fiber. In index-guide fibers, light, like traditional fibers, is guided according to the law of general internal reflection in the core region. Because the interaction of light with the gas sample inside the core is increased, so the sensitivity of these fibers compared to index-guide fibers is significant [5-7].

PCFs with different geometry give a specific relative sensitivity. These PCFs have various geometry, such as hexagon [8], octagonal [2], decagonal [9], and circular [10]. PCFs can be used for several applications such as spectroscopy [11], nonlinear optics [12], high power technology [13], and sensor [14].

In [15], the author shows that placing hexagonal holes instead of circular holes in the innermost ring is increased the relative sensitivity to 13.23% at 1.33µm wavelength. A micro-structured core and cladding PCF has been reported with a relative sensitivity of 42.27% [16]. They showed that increasing the diameter of air holes in the microstructure core enhances the relative sensitivity [16]. Furthermore, a PCF has been proposed with a high relative sensitivity of 53.07% at  $\lambda=1.33\mu m$  [17]. Finally, in [18], the author proposed a new

circular PCF with a high sensitivity of 72.01% at the wavelength of 1.33µm.

In this article, a new triangular PCF with high sensitivity and low confinement loss has been proposed. The numerical results show that our proposed sensor gives the highest relative sensitivity at the wavelength of 1.33µm. Due to the high sensitivity, birefringence, and effective area of our structure, it can be fabricated as a gas sensor for medical and industrial applications.

### II. Proposed PCF based geometrics

Figure 1 shows the cross-section of the proposed PCF in which the cladding contains two triangular layers, and the core contains a hexagonal layer with a central hole that surrounded them. The diameter of the layers in the cladding region is defined by the d parameter. The diameter of the hexagon holes and the central hole in the core region is defined by  $d_{c2}$  and  $d_{c1}$  parameters. The distance between the centers of two adjacent holes is called the pitch. The amount of pitch in the cladding region is defined by the  $\Lambda$  parameter. The parameter of the pitch in the core region for the hexagon layer is determined by the  $\Lambda_{cl}$ . Table. I shows the value of these parameters. The perfectly matched layer of the proposed PCF is adjusted around 10% for absorbing the light-wave [4].

VOL. 9, NO. 1, JANUARY 2021



TABLE I. The value of the proposed PCF parameters

$\text{VALUE}\left(\mu m\right)$
1.6
0.52
0.52
1.8
0.53

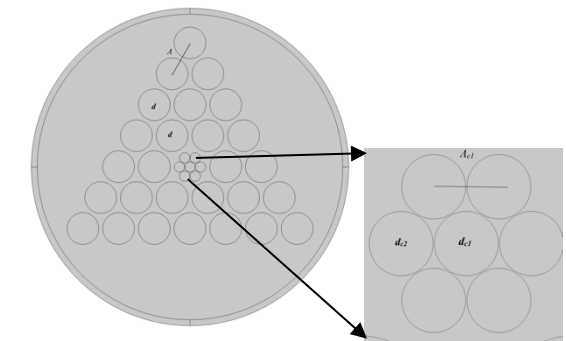


FIGURE 1. Transverse cross section of the proposed PCF.

## III. Mathematical equations and numerical analysis

Because of the high accuracy and reliability of the finite element method (FEM), this technique is used for analyzing the proposed gas sensors [2, 7, 15]. The relative sensitivity and confinement loss are two critical parameters that should be investigated for PCFs. The variation of holes and the number of layers in the cladding or core region can change these parameters. The relative sensitivity is obtained from the interaction of the light and gas samples. The higher value of this parameter shows that the PCF can detect more gas sample precisely. Confinement loss indicates the leakage of guided light, which spread into the PCF. It can be calculated by the following equation [15-18]:

$$L_c = 8.686 \times k_0 \times \text{Im} \left[ n_{eff} \right] \left( \frac{dB}{m} \right)$$
 (1)

Here,  $I_m[n_{eff}]$  and  $k_0$  are the imaginary part of the effective index and the wavenumber, respectively. The optical intensity is obtained by the Lambert-beer law and can be expressed as [16]:

$$I(\lambda) = I_0(\lambda) \exp(-r\alpha_m lc)$$
 (2)

Here, l is the length of the PCF, c is the gas concentration,  $I(\lambda)$  and  $I_0(\lambda)$  are the input and output intensities,  $\alpha_m$  is the gas absorption coefficient, and r is a relative sensitivity coefficient, which can be defined as [16]:

2

$$r = \frac{n_s}{Re[n_{eff}]} f \tag{3}$$

Here,  $Re[n_{eff}]$  is the real part of the effective mode index, and  $n_s$  is the refractive index of gas species considered 1. The divide of total power and holes power is defined by f, which can be calculated by the following equation [16-18]:

$$f = \frac{\int_{hole} Re(E_x H_y - E_y H_x) dx dy}{\int_{total} Re(E_x H_y - E_y H_x) dx dy}$$
(4)

Here,  $E_x$  and  $H_x$  are the transverse electric and magnetic fields of mode,  $E_y$  and  $H_y$  are the longitudinal electric and magnetic fields of mode.

Birefringence is another critical property of PCF, which is used in polarization applications [19]. Birefringence happens because of moving the fundamental electromagnetic modes with different velocities, which have variant refractive indices [19]. This parameter is calculated by subtracting the refractive index of x-polarization and y-polarization of fundamental electric field modes, which can be defined [19]:

$$B = \mid n_x - n_y \mid \tag{5}$$

The effective area  $(A_{eff})$  of a PCF can be specified by the following equation [20]:

$$A_{eff} = \frac{\left(\iint |E|^2 dx dy\right)^2}{\iint |E|^4 dx dy} \tag{6}$$

The background material was set pure silica whose refractive index alters with the change of the wavelength according to the Sellmeier equation.

$$n(\lambda) = \sqrt{1 + \frac{B_1 \lambda^2}{\lambda^2 - C_1} + \frac{B_2 \lambda^2}{\lambda^2 - C_2} + \frac{B_3 \lambda^2}{\lambda^2 - C_3}}$$
(7)

Here,  $n(\lambda)$  is the refractive index of silica, which changes with the operating wavelength, and  $B_{(i=1,2,3)}$  and  $C_{(i=1,2,3)}$  are Sellmeier coefficients [20].

#### IV. Simulation Results and Discussion

Figure 2 shows the 2D views of fundamental Electric field distribution at 1.33µm. The FEM has been used for analyzing numerical results. The size of the mesh is normal and solved by physics controlled mesh, which gives the number of degrees of freedom for 82773. It can be seen that the core region indicates the highest electric field at the 1.33µm wavelength, which gives the relative sensitivity as high as 75.14%. The sample gas is filled in the core region. The results show that the PCF has high birefringence and

VOL. 9, NO. 1, JANUARY 2021

effective area of the order  $3.75 \times 10^{-3}$  and  $14.07 \mu m^2$  and also low confinement loss of  $1.41 \times 10^{-2}$  dB/m. Figures 3a and 3b show the relative sensitivity and confinement loss of the proposed PCF from  $1.1 \mu m$  to  $1.7 \mu m$  wavelengths. All holes are filled with air with a refractive index of 1. Both relative sensitivity and confinement loss is increased from wavelengths  $1.1 \mu m$  to  $1.7 \mu m$ .

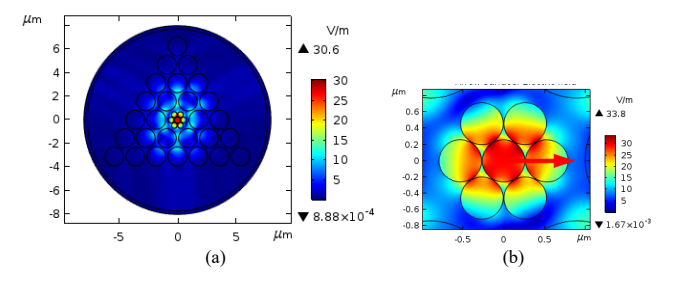
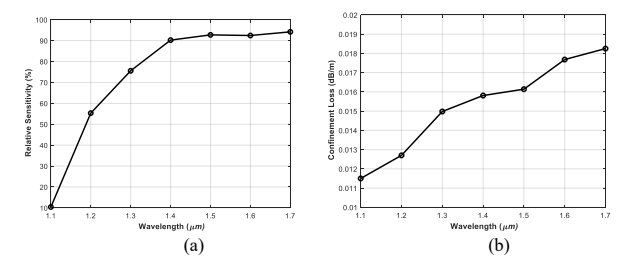
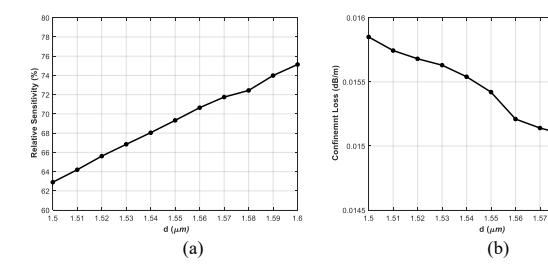


FIGURE 2. 2D view of Mode field pattern of proposed PCF for x-polarization at 1.33μm wavelength for (a) whole and (b) core region.



**FIGURE 3.** a) The relative sensitivity and b) the confinement loss of Proposed PCF for wavelengths around  $1.1\mu m$  to  $1.7\mu m$ .

The variation of the diameter and the pitch may change the relative sensitivity and confinement loss of the proposed PCF. Therefore, these parameters should be investigated. There is always a trade-off between the relative sensitivity and confinement loss. The d,  $d_{c1}$ , and  $d_{c2}$  parameters have been changed, respectively, while the other ones are kept constant. As it is seen from Figures 4a and 4b, the diameter d in the cladding region has a significant effect on both relative sensitivity and confinement loss. Because this structure has only two layers in the cladding region, and they are close to the core region, it is expected that the variation of the d parameter affects the sensitivity. To reach the highest sensitivity, we choose a bigger value for this layer, and by decreasing the diameter of this parameter, the sensitivity will be decreased. This parameter also controls the confinement loss. As Figure 4b shows. By decreasing the diameter of this parameter, the confinement loss will be increased.



**FIGURE 4.** Variation of a) the relative sensitivity and b) the confinement loss for different values of *d*, while other parameters are kept constant.

The variation of the central hole in the core region is investigated. As shown in Figure 5, by decreasing the diameter of this parameter, the sensitivity will be reduced. This layer indicates a bit of change for both the relative sensitivity and confinement loss parameter. Figure 6 shows the variation of the  $d_{c2}$  parameter in the core region. As can be seen, by decreasing the diameter of  $d_{c2}$ , the sensitivity will be decreased, and the confinement loss will be increased. Because the sample gas will be embedded in the core region, the variation of diameters in the core region mostly affects the relative sensitivity.

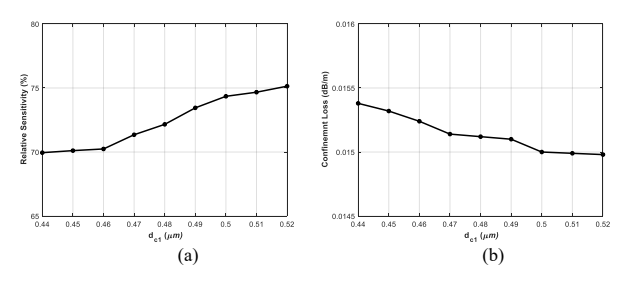


**FIGURE 5.** Variation of a) the relative sensitivity and b) the confinement loss for different values of  $d_{c1}$ , while other parameters are kept constant.

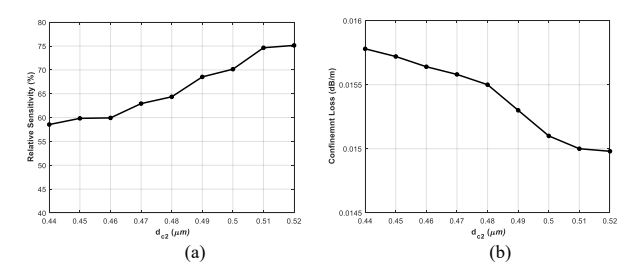


**FIGURE 6.** Variation of a) the relative sensitivity and b) the confinement loss for different values of  $d_{c2}$ , while other parameters are kept constant.

Figure 7 shows the impact of the number of cladding layers on the relative sensitivity and the confinement loss. By increasing the layers to three, the sensitivity will be reduced to 60 %, but the confinement loss will be decreased to  $1.6 \times 10^{-3}$ . Therefore, if the higher relative sensitivity is essential rather than confinement loss, it is better to use two-

layer cladding. But if the confinement loss is important, and the moderate relative sensitivity around 60% is enough, it is better to use three-cladding layers for this triangular structure.

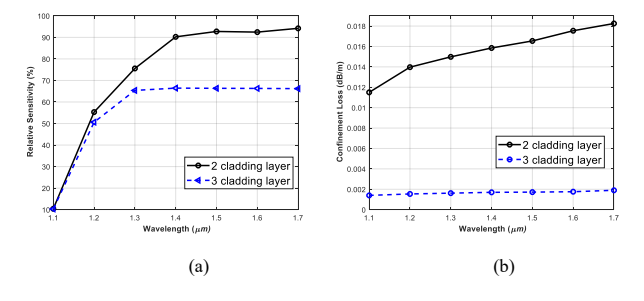
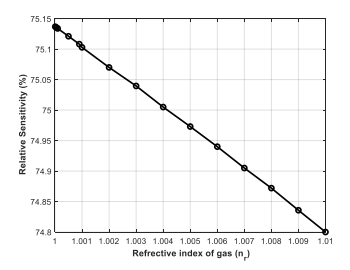


FIGURE 7. Impact of the number of layers on a) the relative sensitivity and b) the confinement loss in the cladding region.

The PCF gas sensors have been reported and investigated at  $\lambda=1.33\mu m$ , which is the absorption line of the methane gas for detecting air pollution in the literature. The proposed PCF in this article shows the highest relative sensitivity rather than other PCFs. Table II exhibits a comparison between the PCFs reported in the literature at  $\lambda$ =1.33 $\mu$ m. From the comparison, it may be seen that our suggested PCF gives the highest relative sensitivity and effective area rather than other PCFs at a wavelength of 1.33 µm. Figure 8 shows the effect of the gas refractive index on the relative sensitivity of the proposed structure at  $\lambda=1.33\mu m$ . Because the refractive index of most gases is between  $1+(1\times10^{-5})$  to  $1+(1\times10^{-2})$ , and the proposed sensor shows the highest sensitivity in these values, it will show good performance in detecting gases. It may be seen from Figure 8 that, by increasing the gas refractive index, the relative sensitivity is decreased. By increasing the refractive index of gas, the velocity of light is decreased, and the power of light in the core region will be decreased, which makes the relative sensitivity be decreased.

**TABLE II.** Comparison between the reported relative sensitivity with PCFs in the literature at  $\lambda$ =1.33 $\mu$ m.

PCFs		SENSITIVITY (%)	$A_{eff}(\mu m^2)$
Ref [15]	13.23		-
Ref [16]	42.27		-
Ref [17]	53.07		3.88
Ref [18]	72.04		10.04
Proposed PCF	75.14		14.07



**FIGURE 8.** Variation of the relative sensitivity with the refractive index of gas.

The proposed PCF is formed with a shaped triangular air hole in the cladding region and a hexagonal microstructure hole in the core region. The fabrication process of this PCF may not be easy spatially for the core region. However, the fast technological development helps overcome the fabrication challenges. There are some methods for the construction of PCFs, such as stack and draw [21], drilling [22], Sol-gel casting [23], and extrusion [12] methods. In [23], they have suggested a sol-gel technique to build the PCFs with high degrees of freedom to adjust the air-hole shape, size, and spacing. In such a situation, the sol-gel casting method gives design flexibility to build our proposed PCF.

### V. CONCLUSION

In this paper, a new triangular PCF with a hexagonal layer and a central hole surrounding them has been presented. The finite element method is used for solving numerical analysis. The variation of the diameters has been investigated and showed that our structure represents good stability for fabrication. The proposed PCF shows 75.14% sensitivity and  $1.41\times10^{-2}$  dB/m confinement loss and high birefringence of  $3.75\times10^{-3}$  at  $\lambda=1.33\mu\text{m}$ , which can be used as a gas sensor for medical and industrial applications.

# **REFERENCES**

- P. Russell, "Photonic crystal fibers," Science, vol. 299, pp. 358-62, Jan 17 2003.
- [2] H. Ademgil, "Highly sensitive octagonal photonic crystal fiber based sensor," *Optik*, vol. 125, pp. 6274-6278, 2014.
- [3] J. M. Fini, "Microstructure fibres for optical sensing in gases and liquids," *Measurement Science and Technology*, vol. 15, p. 1120, June 01, 2004.
- [4] T. A. Birks, J. C. Knight, and P. S. J. Russell, "Endlessly single-mode photonic crystal fiber," *Opt. Lett.*, vol. 22, pp. 961--963, 1997
- [5] Y. L. Hoo, W. Jin, J. Ju, and H. L. Ho, "Numerical investigation of a depressed-index core photonic crystal fiber for gas sensing," *Sensors and Actuators B: Chemical*, vol. 139, pp. 460-465, 2009.
- [6] Z. Zhi-guo, Z. Fang-di, Z. Min, and Y. Pei-da, "Gas sensing properties of index-guided PCF with air-core," *Optics Laser Technology*, vol. 40, p. 167, February 01, 2008.
- [7] M. B. C. Cristiano, A. R. F. Marcos, C. Giancarlo, C. S. B. Elaine, L. Richard, C. H. B. Cruz, et al., "Microstructured-core optical fibre for evanescent sensing applications," Opt. Express, vol. 14, pp. 13056--13066, 2006.
- [8] J. C. Knight, T. A. Birks, P. S. J. Russell, and D. M. Atkin, "All-silica single-mode optical fiber with photonic crystal cladding: errata," *Optics Letters*, vol. 22, pp. 484-485, 1997/04/01 1997.
- [9] S. M. A. Razzak, N. Yoshinori, K. Md. Abdul Goffar, F. Begum, and S. Kaijage, "GUIDING PROPERTIES OF A DECAGONAL PHOTONIC CRYSTAL FIBER," Journal of Microwaves, Optoelectronics and Electromagnetic Applications (JMOe), vol. 6, pp. 44-49, 2007.
- [10] S. Asaduzzaman, M. F. H. Arif, K. Ahmed, and P. Dhar, "Highly sensitive simple structure circular photonic crystal fiber based

VOL. 9, NO. 1, JANUARY 2021

- chemical sensor," in 2015 IEEE International WIE Conference on Electrical and Computer Engineering (WIECON-ECE), 2015, pp. 151-154.
- [11] R. Holzwarth, T. Udem, T. W. Hänsch, J. C. Knight, W. J. Wadsworth, and P. S. J. Russell, "Optical Frequency Synthesizer for Precision Spectroscopy," *Physical Review Letters*, vol. 85, pp. 2264-2267, 2000.
- [12] H. Ebendorff-Heidepriem, P. Petropoulos, S. Asimakis, V. Finazzi, R. C. Moore, K. Frampton, et al., "Bismuth glass holey fibers with high nonlinearity," Optics Express, vol. 12, pp. 5082-5087, 2004.
- [13] C. Lecaplain, B. Ortaç, G. Machinet, J. Boullet, M. Baumgartl, T. Schreiber, et al., "High-energy femtosecond photonic crystal fiber laser," Optics Letters, vol. 35, pp. 3156-3158, 2010.
- [14] M. Morshed, S. Asaduzzaman, M. F. H. Arif, and K. Ahmed, "Proposal of simple gas sensor based on micro structure optical fiber," in 2015 International Conference on Electrical Engineering and Information Communication Technology (ICEEICT), 2015, pp. 1-5.
- [15] S. Olyaee, A. Naraghi, and V. Ahmadi, "High sensitivity evanescent-field gas sensor based on modified photonic crystal fiber for gas condensate and air pollution monitoring," *Optik*, vol. 125, p. 596, January 01, 2014.
- [16] M. Morshed, M. Imran Hassan, T. K. Roy, M. S. Uddin, and S. M. Abdur Razzak, "Microstructure core photonic crystal fiber for gas sensing applications," *Applied Optics*, vol. 54, pp. 8637-8643, 2015.
- [17] S. Asaduzzaman and K. Ahmed, "Proposal of a gas sensor with high sensitivity, birefringence and nonlinearity for air pollution monitoring," *Sensing and Bio-Sensing Research*, vol. 10, pp. 20-26, 2016.
- [18] A. S. H. Rabee, M. F. O. Hameed, A. M. Heikal, and S. S. A. Obayya, "Highly sensitive photonic crystal fiber gas sensor," *Optik*, vol. 188, pp. 78-86, 2019.
- [19] M. T. Anas, S. Asaduzzaman, K. Ahmed, and T. Bhuiyan, "Investigation of highly birefringent and highly nonlinear Hexa Sectored PCF with low confinement loss," Results in Physics, vol. 11, pp. 1039-1043, 2018.
- [20] M. Ibadul Islam, K. Ahmed, S. Asaduzzaman, B. K. Paul, T. Bhuiyan, S. Sen, et al., "Design of single mode spiral photonic crystal fiber for gas sensing applications," Sensing and Bio-Sensing Research, vol. 13, pp. 55-62, 2017.
- [21] J. Broeng, D. Mogilevstev, S. E. Barkou, and A. Bjarklev, "Photonic Crystal Fibers: A New Class of Optical Waveguides," Optical Fiber Technology, vol. 5, pp. 305-330, 1999.
- [22] M. N. Petrovich, A. v. Brakel, F. Poletti, K. Mukasa, E. Austin, V. Finazzi, et al., "Microstructured fibres for sensing applications," in *Proc.SPIE*, 2005.
- [23] T. B. Ryan and J. T. Dennis, "Sol-gel Derived Microstructured Fiber: Fabrication and Characterization," Optical Fiber Communication Conference and Exposition and The National Fiber Optic Engineers Conference, p. OWL6, 2005.